International Journal of Applied Engineering Research ISSN 0973-4562 Volume 13, Number 9 (2018) pp. 6569-6578

Tool Specifications Effect on the Generated Heat during Friction Stir Welding Process

Sadiq Aziz Hussein* **Adil Kadhim Mashaf** **Sameer Hashim Ameen**

Technical Instructors Training Institute, Middle Technical University - Baghdad- Iraq.
**Correspondence Author*

Abstract

Solid-state, friction stir welding, is an efficient joining method of a wide range of similar and dissimilar materials. Heat is generated by a rotated tool along the abutting line of the workpieces to be welded. Therefore, the tool specification represents a pivotal factor during the welding process. This study aimed to evaluate the tool materials, tool tilt angle, and tool size effects on the generated heat during the friction stir welding process of AA7075. The welding parameters; rotational and welding speeds were kept constant. Analysis of variance and finite element method were carefully implemented to obtain the results. The results showed that the pin size plays a main role in heat generation process and cannot be neglected as suggested by some other studies. The maximum modeled temperature can attain 658 °C when the pin and shoulder diameters were 8 mm and 15 mm, respectively, while the tilt angle was 3°. Decreasing the pin diameter to 4 mm with same values of the two other factors promoted 502 °C.

Keywords: FSW, FEM, tool design, tool materials, tilt angle, temperature distribution.

INTRODUCTION

In the last three decades, the emerging friction stir welding (FSW) has been addressed as a significant contribution in metal joining process. Since it is environmentally friendly, energy efficient, and versatile, therefore, it can be assumed as the new Green Technology in welding field [1]. FSW offers many significant advantages as compared to the commonly traditional fusion welding methods [2]. The FSW tool could be worn-out due to the associated forces, friction and heat [3,4]. However, the resulted heat has a very important role in the plasticization incident of material during the welding process.

One of the extremely important purposes of the FSW tool is to generate an adequate heat during the welding process. This heat is highly contributed to the tool wear incident as well. Therefore, the heat models and temperature distribution of FSW process are well discussed in many available studies. For instance, Frigaard et al. developed a finite difference thermal model that explains the relationship of the generated heat regarding various welding parameters during FSW process [5]. According to their model; heat is relational to the rotational speed and shoulder diameter. Ulysse adopted a visco-plastic model, a similar model was suggested by Nandan et al. for the thermo-mechanical modeling, and both models could inspect the temperature distribution and viscous material flow [6, 7]. The finite elements method (FEM) of FSW deemed an efficient tool to simulate the associated heat and temperature distribution. Besides, FEM provides a better understanding of the metal flow patterns during the welding process. Hence, many software have been used as discussed by He et al. [8].

Tool materials that generally used to weld low strength materials are usually made from various steel grades such as H13 steel. Tungsten-based alloys and cobalt (Co) alloys are used for FSW of high strength materials. Some other tool made of tungsten carbide (WC) is also effectively used. Poly cubic boron nitride (PCBN) is preferred to weld hard alloys such as steel, copper and titanium alloys because of its mechanical and thermal properties [9, 10].

So far, selection procedure of an adequate FSW tool before welding still not clearly demonstrated in the related literature. Some studies examine the tool specifications effect on the related heat in a discriminatory scheme. In this study, an investigation on the conjointly effects of tool: material, tilt and size on the final generated heat.

Description of the model

Different finite element software have been carried out to evaluate the temperature distribution of the FSW [11]. In the present study, the simulation was carried out by using Altair HyperWorks™ software which is developed by *Altair Engineering*. HyperWorks can be efficiently used for many modules in; visualization, manufacturing solutions, structural optimization and engineering solutions. Recently, many studies using this software for the FSW simulation [12, 13]. The mass flow of material was assumed to behave as incompressible non-Newtonian and visco-plastic, this assumption is agreed by Nandan et al [7].

The continuity equation for incompressible single-phase flow is explained in index notation for *i* equal to 1, 2, and 3 which representing x, y, and z directions respectively is [7]:

$$\frac{\partial u_i}{\partial x_i} = 0 \qquad \ldots\ldots (1)$$

where *u* is the plastic flow velocity. Therefore, the steady single phase momentum conservation equations can be written as [7]:

$$\rho \frac{\partial u_i u_j}{\partial x_i} = -\frac{\partial P}{\partial x_j} + \frac{\partial}{\partial x_i}\left(\mu \frac{\partial u_j}{\partial x_i} + \mu \frac{\partial u_i}{\partial x_j}\right) - \rho v \frac{\partial u_i}{\partial u_j} \qquad \ldots\ldots (2)$$

where ρ, μ, v and P; are the density, the dynamic viscosity, the travel velocity and the pressure of the plastic flow, respectively. The viscosity was considered based on the next flow stress formulation [7]:

$$\sigma_e = \frac{1}{\alpha} sinh^{-1}[(\frac{Z}{A})^{\frac{1}{n}}] \quad \ldots\ldots (3)$$

The Z value can be calculated as follow:

$$Z = \dot{\varepsilon} exp\left(\frac{Q}{RT}\right) \quad \ldots\ldots (4)$$

where σ_e is the flow stress, Z is Zener-Hollomon parameter, while α, A and n are material constants. Q and R are the temperature independent activation energy and the gas constant, respectively. $\dot{\varepsilon}$ is the effective strain rate which is:

$$\dot{\varepsilon} = \left(\frac{2}{3}\ \varepsilon_{ij}\varepsilon_{ij}\right)^{1/2} \quad \ldots\ldots (5)$$

The stress flow and effective strain rate can be used to determine the viscosity:

$$\mu = \frac{\sigma_e}{3\dot{\varepsilon}} \quad \ldots\ldots (6)$$

The thermal properties and other constants are shown in Table 1.

The model dimensions are shown in Figure 1. The element type which selected for the present analysis was 3D Hexahedral with 20 nodes. The element was 3 degrees of freedom and serves both mechanical and thermal analysis. The isometric view of the developed model with final mesh is shown in Figure 2. The strain calculation of the FEM modeling implemented the *Galerkin's* weighted residual method. The strain rate curves with viscosity and flow stress are shown in Figures 2 and 3, respectively.

Table 1: Constants of the numerical model

Property	**value**
Density (Kg/m^3)	2810
Specific heat (J/Kg.K)	960
Thermal conductivity (W/m.K)	173
Coeff. of thermal Expan. (1/K)	1e-005
Stress exponent	5.41
A: Reciprocal strain factor (1/sec)	1.027094727e+09
α (1/MPa)	0.0141
Strain rate offset (1/sec)	0.0001
Activation energy (J/mol)	129400
Universal gas constant (J/mol.K)	8.314

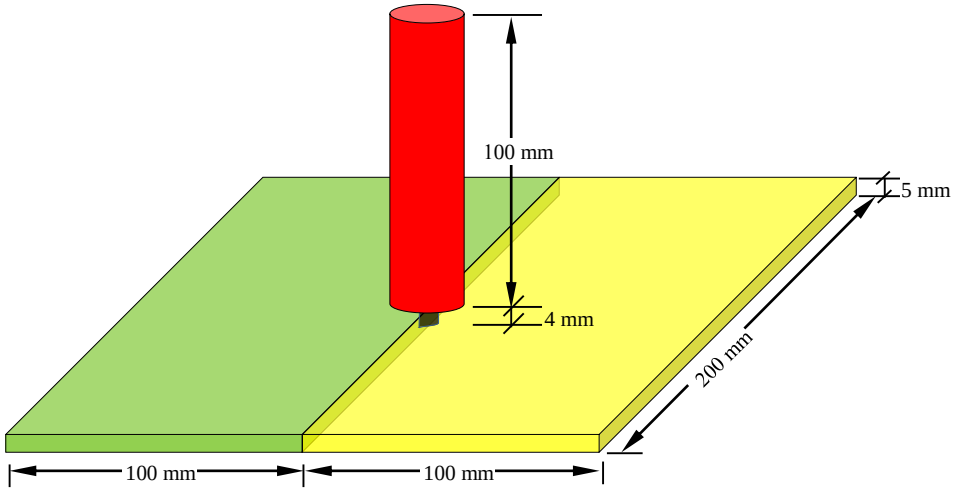

Figure 1: Schematic diagram of the FSW

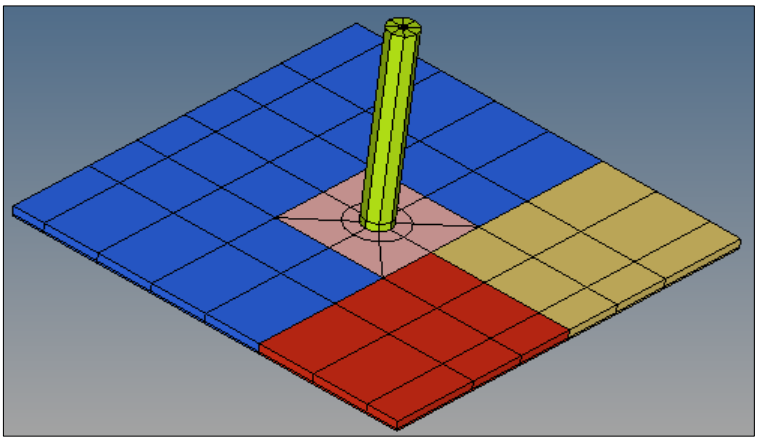

Figure 2: Mesh of the finite element model.

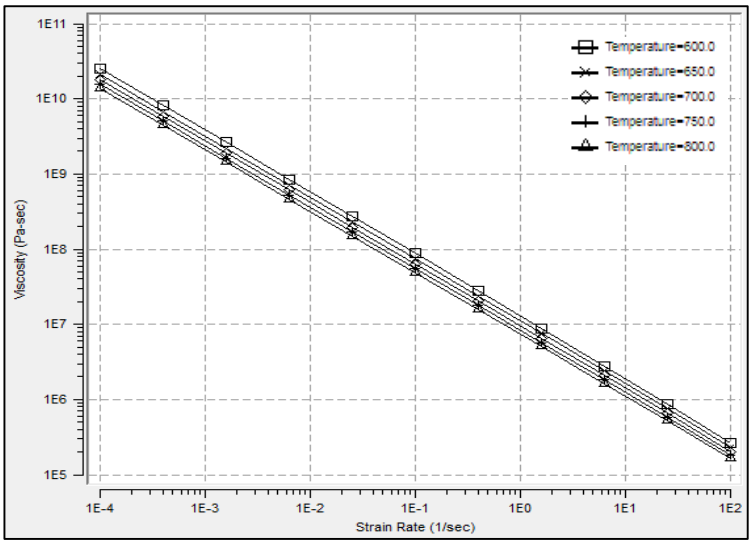

(a)

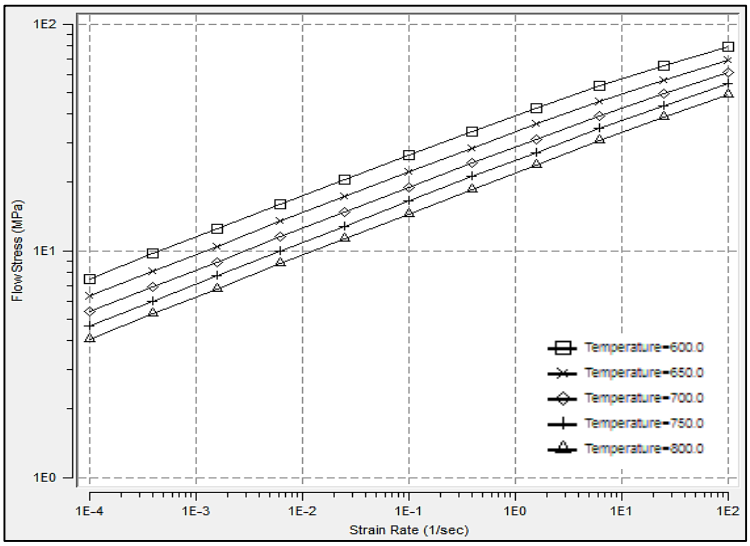

(b)

Figure 3: Relation of strain rate contours for various temperatures and (a) viscosity, (b) flow stress, of AA7075 material [14].

The Factorial Analysis of Variance (ANOVA) was employed to analyze the resulted data. Table 2 explains the factors levels while the rotational and welding speeds were kept constant.

Table 2: Full Factorial levels

Factor	Levels		
	-1	**0**	**+1**
Shoulder diameter (DS) mm	10	12.5	15
Pin diameter (DP) mm	8	6	4
Tilt angle (TA) degree	0	1.5	3

RESULTS AND DISCUSSION

The resulted temperature profiles of different process parameters along the tool axes and through the workpiece are shown in Figures 4 and 5. So far, the temperature values are agreed with the literature [8, 7, 15]. It is clear that the heat on the top surface of the workpiece is transported to the material that already preheated behind the tool. However, the maximum temperature profiles were within the plunging zone. Figure 4 shows the effect of tilt angle while Figure 5 shows the effect of the shoulder diameter. The effect of pin diameter is shown in Figures 4 (b) and 5 (a). Yet, it is evident that the dominated process parameter is not very clear. Therefore, the statistical method would be the helpful tool to explain the results. Therefore, the resulted temperatures were collected in a factorial matrix (Table 3) to do the statistical analysis.

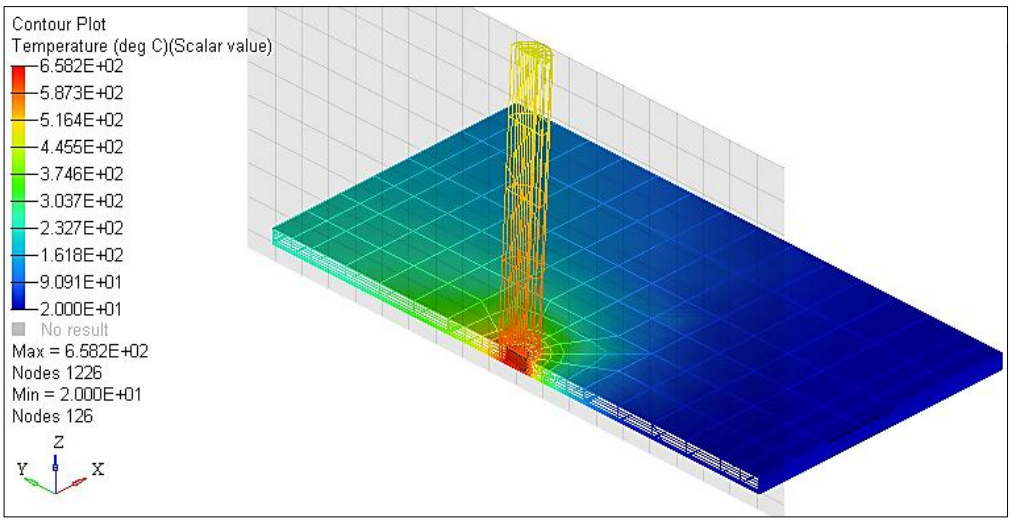

(a)

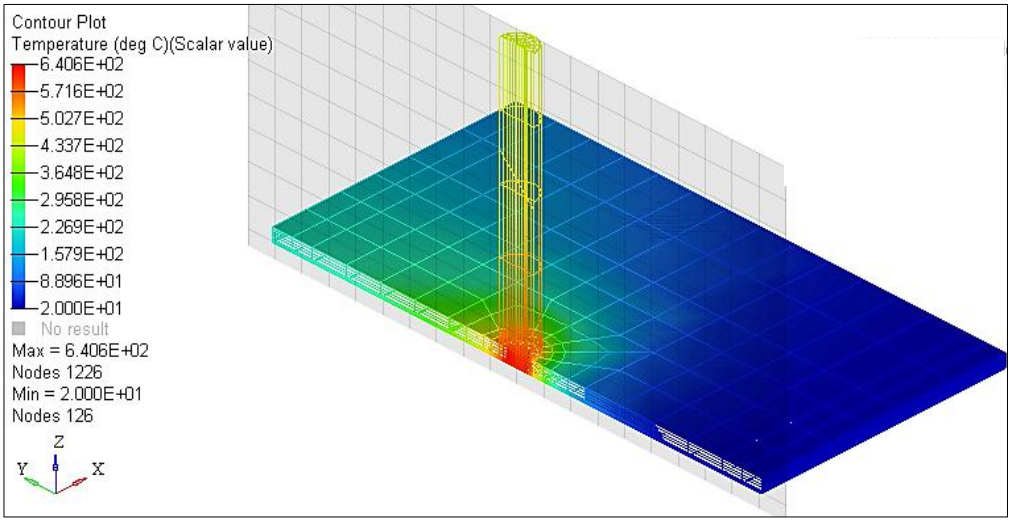

(b)

Figure 4: Effect of tilt angle on the resulted temperature; (a) DS is 15 mm, DP is 8 mm, and TA is 3°, and (b) DS is 15 mm, DP is 8 mm, and TA is 0°.

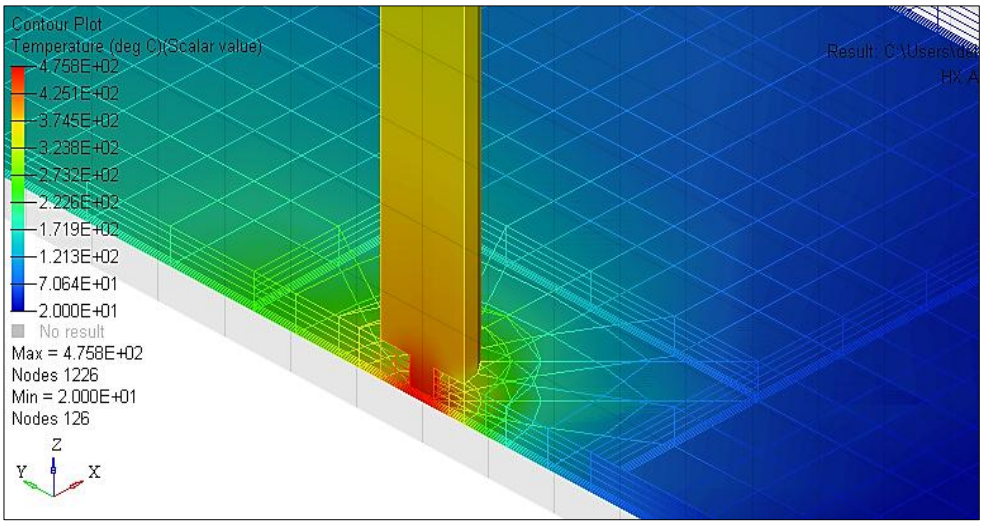

(a)

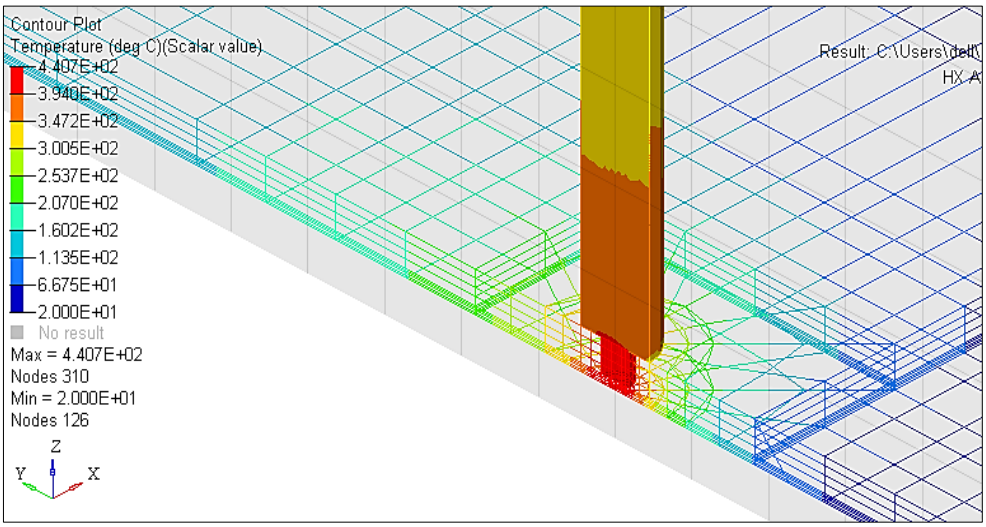

(b)

Figure 5: Effect of shoulder diameter on the resulted temperature; (a) DS is 15 mm, DP is 4 mm, and TA is 0°, and (b) DS is 10 mm, DP is 4 mm, and TA is 0°.

Table 3: Full Factorial data matrix

StdOrder	RunOrder	PtType	Blocks	DS (mm)	DP (mm)	TA (deg)	Tp (°C)
10	1	1	1	15	4	0	475.8
4	2	1	1	10	6	0	535.5
20	3	1	1	12.5	4	1.5	470.7
13	4	1	1	15	6	0	564.4
25	5	1	1	12.5	8	0	633.1
27	6	1	1	12.5	8	3	648.8
3	7	1	1	10	4	3	461.2
17	8	1	1	15	8	1.5	645.4
26	9	1	1	12.5	8	1.5	636.7
12	10	1	1	15	4	3	501.8
21	11	1	1	12.5	4	3	487.3

StdOrder	RunOrder	PtType	Blocks	DS (mm)	DP (mm)	TA (deg)	Tp (°C)
2	12	1	1	10	4	1.5	445.2
8	13	1	1	10	8	1.5	626.8
1	14	1	1	10	4	0	440.7
6	15	1	1	10	6	3	551.8
19	16	1	1	12.5	4	0	463.4
23	17	1	1	12.5	6	1.5	558.6
7	18	1	1	10	8	0	624.5
15	19	1	1	15	6	3	585.8
9	20	1	1	10	8	3	639.3
5	21	1	1	10	6	1.5	538.1
16	22	1	1	15	8	0	640.6
14	23	1	1	15	6	1.5	570.8
24	24	1	1	12.5	6	3	573
22	25	1	1	12.5	6	0	553.6
18	26	1	1	15	8	3	658.2
11	27	1	1	15	4	1.5	484.5

Table 3 Continued….

The AVOVA indicated that all selected parameters of this study were significantly affected the results since the P-values were below the significant value (0.05) as shown in Tables 4 & 5. However, the more significant effect was the pin diameter as shown in Figures 6 and 7. Figure 6 shows the slop of the main effect plot of the selected factors. The slop of the pin diameter (DP) is more effective than the shoulder diameter (DS) and the tilt angle (TA) factors effects. The contour plot of the ANOVA plot Figure 7 demonstrates that increasing DS and TA is contributing to the DP effect on the resulted temperature Figure 7 (a and b) shows these effect. On the other side, increasing DS and TA have the lower significant effect (Figure 7-c) since the change in the contour plot shows low sensitivity to the change of both values on the final generated heat.

Table 4: Two-way ANOVA: Tp (°C) versus DS (mm); DP (mm)

Source	DF	SS	MS	F	P
DS (mm)	2	3945	1972.3	18.61	0.000
DP (mm)	2	128945	64472.5	608.30	0.000
Interaction	4	357	89.2	0.84	0.517
Error	18	1908	106.0		
Total	26	135154			

Table 5: Two-way ANOVA: Tp (°C) versus TA (deg); DP (mm)

Source	DF	SS	MS	F	P
TA (deg)	2	1848	923.8	3.85	0.041
DP (mm)	2	128945	64472.5	268.68	0.000
Interaction	4	42	10.5	0.04	0.996
Error	18	4319	240.0		
Total	26	135154			

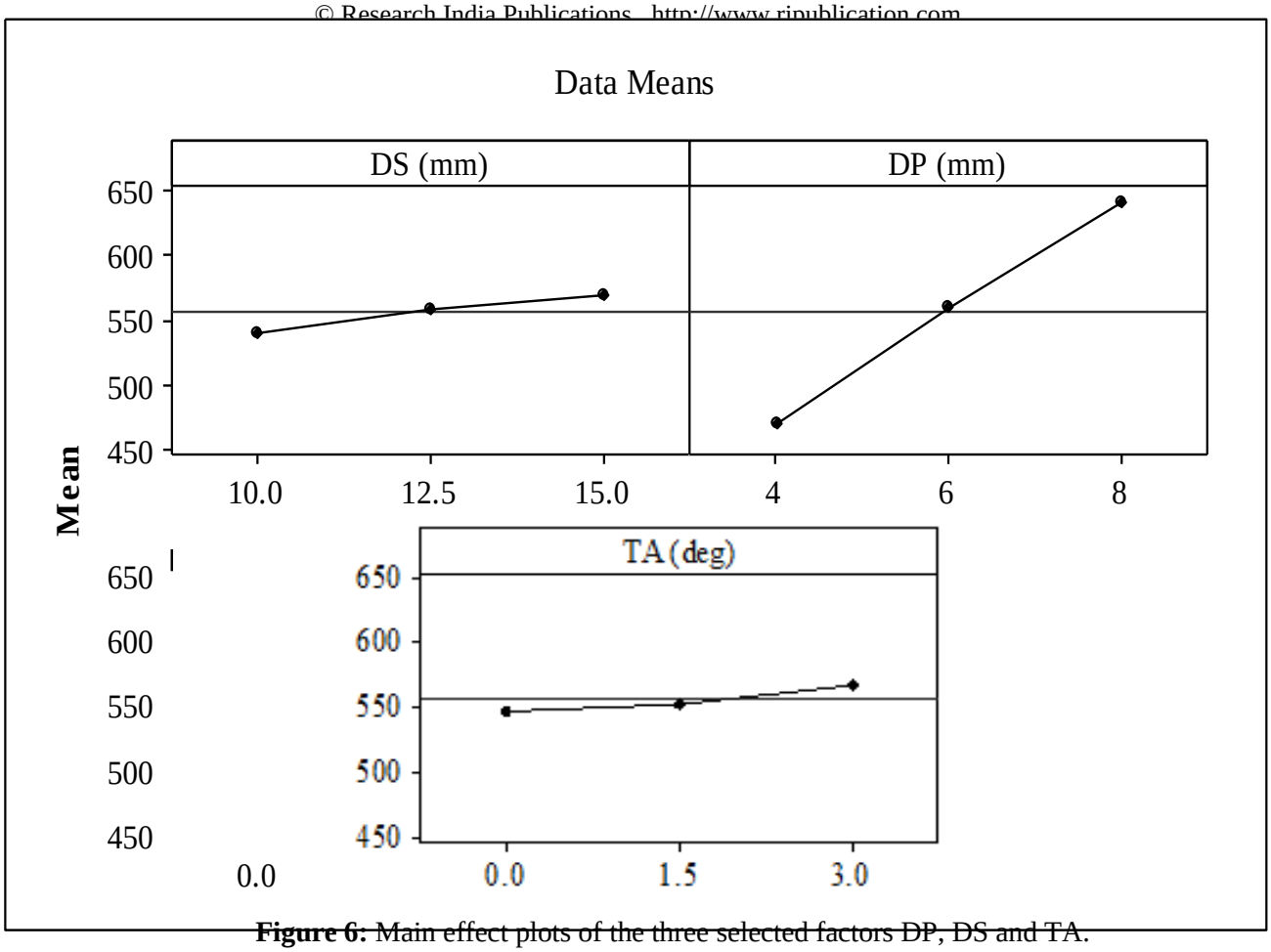

Figure 6: Main effect plots of the three selected factors DP, DS and TA.

The interaction plot, Figure 8, indicates the effect of each parameter on the other one. No intersection lines can be observed within the DP-DS and DP-TA plots. The DS-TA plot demonstrates more feasible interaction especially when the TA is larger than 1.5°. Chen et al reported that the tool tilt angle has a considerable influence on the generated heat during the FSW process [16].

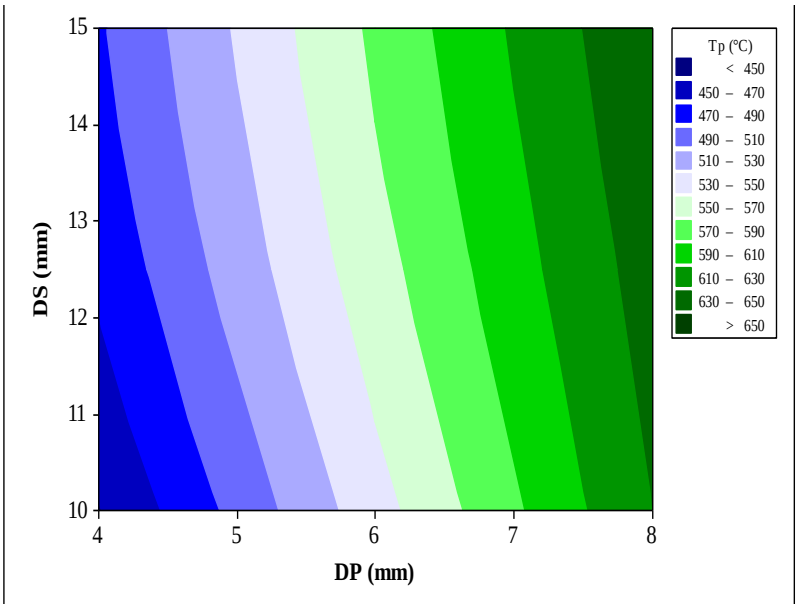

(a)

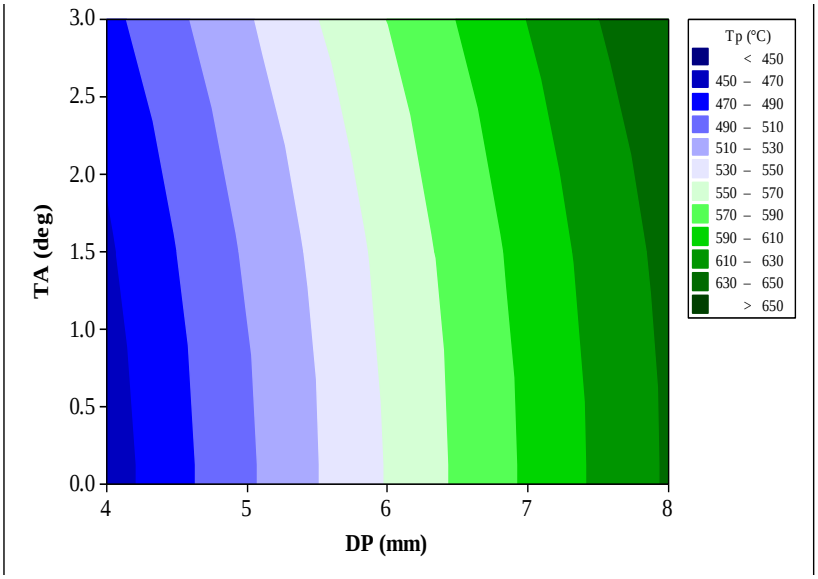

(b)

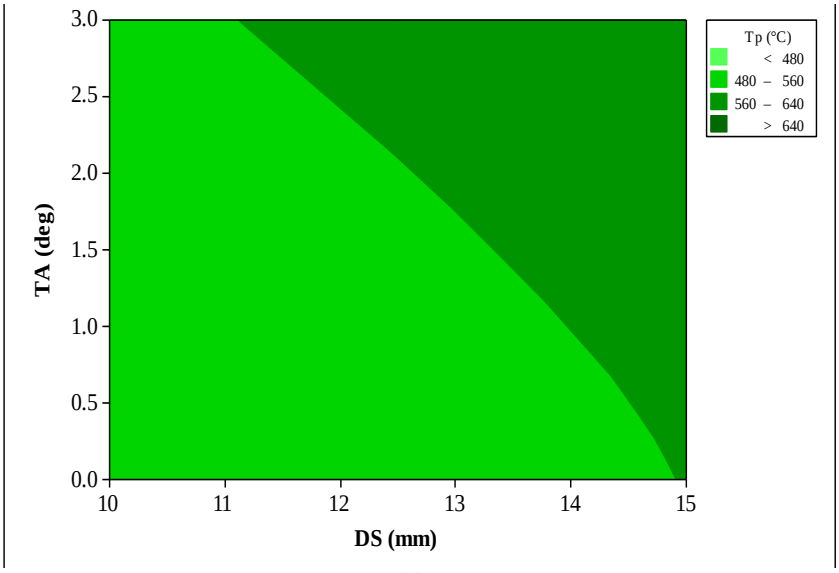

(c)

Figure 7: Contour plots of the statistical analysis; (a) DP-DS (b) DP-TA and (c) DS-TA.

The predicated regression equation of the present model is as follow:

$$Tp\ (°C) = 219 + 5.87\ DS\ (mm) + 42.3\ DP\ (mm) + 6.50\ TA° \quad \ldots\ldots\ldots(7)$$

In general, the accommodation of adequate stirring process meets the pin size and profile which generate the heat due to the associated plastic deformation. Besides, the contact area of large pin diameter size is greater than the small one which increases the heat further. Therefore, this pin size factor is expected to highly contribute to the heat input during the FSW process, and hence, the pin subjected to wear incident [4]. Many other studies refer to the pin design effect on the generated heat that particularly resulted from material plasticization [17, 18, 19]. Besides, Hussein et al were experimentally approved that the generated force is increased when the pin diameter was increased. They also refer to the associated heat which caused by such factor [20]. The axial force is the responsible factor of the plunge depth of the FSW tool, sufficient axial force is important to attain good weld. The degree of material intermixing and diffusion as well as the material flow patterns are highly depend on flow stress, welding temperature and applied forces [17].

The tool materials effect on the generated heat was investigated in this study as well. Figure 9 explains the obtained results. Obviously, the tool material dose not significantly affect the generated heat of the present model. Nevertheless, the tool material could be the dominated parameter of the wear incident and tensile results [21].

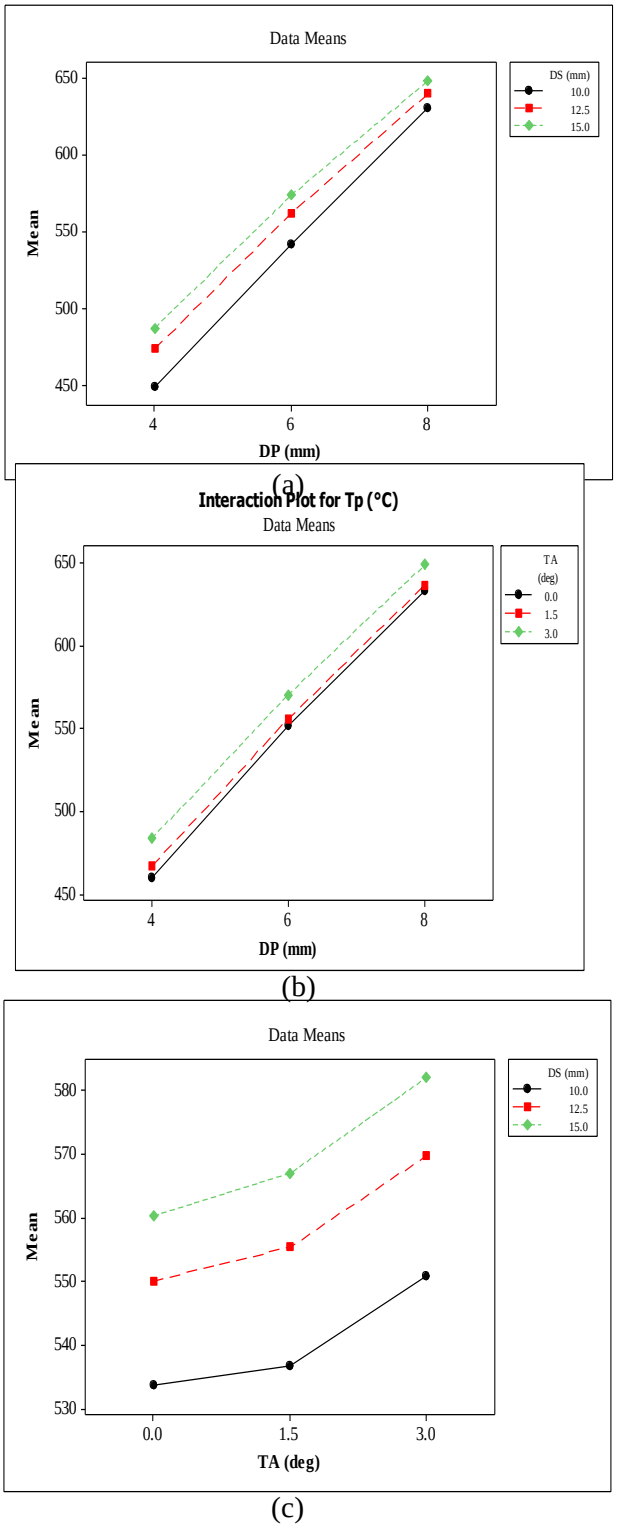

Figure 8: Interaction plots of the statistical analysis between; (a) DP and DS (b) DP and TA and (c) DS and TA.

CONCLUSION

The present study focused on tool design effect and its related heat during the friction stir welding process on the resulted peak temperature. The generated heat was obtained through a finite element model using Altair HyperWorks™ software. Based on the present model the pin diameter has an essential effect on the resulted peak temperature. When the pin and

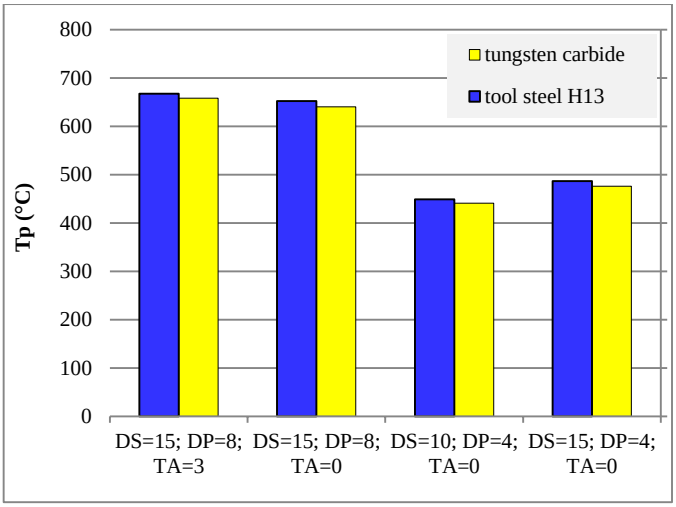

Figure 9: Effect of the tool materials on the resulted peak temperature.

shoulder diameters were 8 mm and 15 mm, respectively, the peak temperature was 658 °C. Decreasing the pin diameter to 4 mm with fixing the other two factors promoted 502 °C. The shoulder and tilt angle factors were also important for the heat generation process. The statistical analysis was used to evaluate the results, and a mathematical model was successfully obtained. Therefore, the study indicates very important issue concerning the neglecting of the pin role on the generated heat in some other related studies. Therefore, the tool size should be carefully selected to attain the required heat during the welding process.

REFERENCES

[1] B. T. Gibson, D. H. Lammlein, T. J. Prater, W. R. Longhurst, C. D. Cox, M. C. Ballun, K. J. Dharmaraj, G. E. Cook, and A. M. Strauss, "Friction stir welding : Process , automation , and control," *Journal of Manufacturing Processes*, vol. 16, pp. 56–73, 2014.

[2] F. C. Liu, Y. Hovanski, M. P. Miles, C. D. Sorensen, and T. W. Nelson, "A review of friction stir welding of steels: Tool, material flow, microstructure, and properties," *Journal of Materials Science & Technology*, vol. In Press, 2017.

[3] M. S. Weglowski, "Friction stir processing – State of the art," *Archives of Civil and Mechanical Engineering*, vol. 18, pp. 114–129, 2018.

[4] J. Wang, J. Su, R. S. Mishra, R. Xu, and J. A. Baumann, "Tool wear mechanisms in friction stir welding of Ti – 6Al – 4V alloy," *Wear*, vol. 321, pp. 25–32, 2014.

[5] Ø. Frigaard, Ø. Grong, and O. T. Midling, "A process model for friction stir welding of age hardening aluminum alloys," *Metallurgical and materials transactions A*, vol. 32A, pp. 1189–1200, 2001.

[6] P. Ulysse, "Three-dimensional modeling of the friction stir-welding process," *International Journal*

of Machine Tools & Manufacture, vol. 42, pp. 1549–1557, 2002.

[7] R. Nandan, G. G. Roy, and T. Debroy, "Numerical Simulation of Three-Dimensional Heat Transfer and Plastic Flow During Friction Stir Welding," *Metallurgical and Materials Transactions A*, vol. 37A, pp. 1247–1259, 2006.

[8] X. He, F. Gu, and A. Ball, "A review of numerical analysis of friction stir welding," *Progress in Materials Science*, vol. 65, pp. 1–66, 2014.

[9] R. Rai, H. K. D. H. Bhadeshia, and T. Debroy, "Review : Friction Stir Welding Tools," *Science and Technology of Welding & Joining*, vol. 16, no. 4, pp. 325–342, 2011.

[10] Y. N. Zhang, X. Cao, S. Larose, and P. Wanjara, "Review of tools for friction stir welding and processing," *Canadian Metallurgical Quarterly*, vol. 51, no. 3, pp. 250–261, 2012.

[11] A. Arif, S. K. Gupta, and K. N. Pandey, "Finite Element Modeling for Validation of Maximum Temperature in Friction Stir Welding of Aluminum Alloy," in *3rd International Conference on Production and Industrial Engineering CPIE-2013*, 2013, no. March 2013, pp. 1087–1094.

[12] Armansyah, I. P. Almanar, M. S. B. Shaari, M. S. Jaffarullah, N. Busu, M. A. F. Zainal, and M. A. A. Kasim, "Temperature Distribution in Friction Stir Welding Using Finite Element Method," *International Journal of Mechanical and Mechatronics Engineering*, vol. 8, no. 10, pp. 1699–1704, 2014.

[13] Y. R. Yatapu, B. R. Reddy, R. V. Ramaraju, M. Faizal, B. Che, and A. Bin Ibrahim, "Prediction of Temperatures during Friction Stir Welding of AA6061 Aluminium Alloy using Hyperworks," *ARPN Journal of Engineering and Applied Science*, vol. 11, no. 18, pp. 11003–11008, 2016.

[14] HyperWorks Manufacturing Solutions, Altair Engineering, Inc.

[15] R. S. Mishra and Z. Y. Ma, "Friction stir welding and processing," *Materials Science and Engineering: R: Reports*, vol. 50, pp. 1–78, 2005.

[16] G. G. Krishna, P. R. Reddy, and M. M. Hussain, "Effect of Tool Tilt Angle on Aluminum 2014 Friction Stir Welds," *Global Journal of Researches in Engineering: JGeneral Engineering*, vol. 14, no. 7, pp. 60–70, 2014.

[17] S. Rajakumar, C. Muralidharan, and V. Balasubramanian, "Influence of friction stir welding process and tool parameters on strength properties of AA7075-T 6 aluminium alloy joints," *Materials & Design*, vol. 32, pp. 535–549, 2011.

[18] H. Schmidt, J. Hattel, and J. Wert, "An analytical model for the heat generation in friction stir welding," *Modelling and Simulation in Materials Science and Engineering*, vol. 12, pp. 143–157, Jan. 2004.

[19] M. Ilangovan, S. R. Boopathy, and V. Balasubramanian, "ScienceDirect Effect of tool pin profile on microstructure and tensile properties of friction stir welded dissimilar AA 6061 e AA 5086 aluminium alloy joints," *Defence Technology*, vol. 11, pp. 174–184, 2015.

[20] S. A. Hussein, A. S. Tahir, and R. Izamshah, "welding and processing †," *Journal of Mechanical Science and Technology*, vol. 29, no. 10, pp. 4319–4328, 2015.

[21] Y. Bozkurt and Z. Boumerzoug, "Tool material effect on the friction stir butt welding of AA2124-T4 Alloy Matrix MMC," *Journal of Materials Research and Technology*, vol. In Press, 2017.